

The Effect of Mellowing and Coal Fly Ash Addition on the Behavior of Sulfate-Rich Dispersive Clay after Lime Stabilization

Nilo Cesar Consoli¹; Eduardo José Bittar Marin²; Rubén Alejandro Quiñónez Samaniego³; Hugo Carlos Scheuermann Filho⁴; Tiago Miranda⁵; and Nuno Cristelo⁶

ABSTRACT: Dispersivity and swelling induced by the formation of expansive minerals are deleterious phenomena that can be observed in natural and treated soils. The former is common among sodium-rich soils that are characterized by the deflocculation of the soil's particles in contact with water. The latter happens due to the growth and hydration of calcium sulfoaluminate minerals as expected in sulphate-rich soils treated with calcium-based stabilizers. The present study assesses the behavior of the Paraguayan sulphate-rich, dispersive as well as expansive, clayey soil after lime stabilization based on an extensive experimental work, which includes unconfined compression, pulse velocity, durability and free swell tests. This work was designed employing a fractional factorial design in the selection of the experimental runs which enabled the statistical evaluation of influence of dry unit weight, lime and fly ash content, curing period, mellowing process and molding moisture content. Results showed that the addition of fly ash, followed by the dry unit weight, were the most influential factors regarding the treated soil's response in performed tests. In addition, mellowing proved to be essential in reducing the volumetric variation verified in the swelling tests. Besides, scanning electron microscopy (SEM) analysis revealed that the ettringite formation was less pronounced when fly ash was added.

Key words: Sulfate; dispersive clay; expansive minerals; lime stabilization; strength; durability; laboratory tests.

¹ Professor of Civil Engineering, Dept. of Civil Engng., Universidade Federal do Rio Grande do Sul, Brazil. E-mail: consoli@ufrgs.br

² Ph.D. Candidate, School of Civil, Environmental and Mining Engineering, The University of Western Australia, Australia. E-mail: bittar.edu@gmail.com (formerly M.Sc. student at Universidade Federal do Rio Grande do Sul, Brazil)

³ Ph.D. Candidate, Dept. of Civil Engineering, Universidade Federal do Rio Grande do Sul, Brazil. E-mail: alejandrorquinonez@ufrgs.br

⁴ M.Sc. Candidate, Dept. of Civil Engineering, Universidade Federal do Rio Grande do Sul, Brazil. E-mail: hugocsf@gmail.com

⁵ Lecturer, Dept. of Civil Engineering, Universidade do Minho, Portugal. E-mail: tmiranda@civil.uminho.pt

⁶ Lecturer, Dept. of Engineering, Universidade de Trás-os-Montes e Alto Douro, Portugal. E-mail: ncristel@utad.pt

30 INTRODUCTION

31

32 The stabilization of dispersive soils through the addition of calcium-based stabilizers, as
33 hydrated lime, has been broadly studied (Hayden and Halliburton 1976; Umesha et al. 2009;
34 Vakili et al. 2012; Consoli et al. 2016; Premukar et al. 2016). However, when soils combine the
35 dispersivity characteristics with high sulphate contents, the stabilization process becomes
36 significantly more complicated. This is the case of the Paraguayan region of Chaco that presents
37 soils with dispersive and expansive characteristics, causing several damages on infrastructures
38 (Fig. 1), especially on road embankments, which require constant maintenance through
39 palliative solutions. Furthermore, the lack of granular materials in this region aggravates the
40 situation because the in situ existing clayey soils are one of the few options available which
41 imply, besides the problematic features of this soil, in poorly graded road embankments.

42

43 The dispersivity phenomenon is characterized by the deflocculation of soil particles in presence
44 of relatively pure water, which implies high susceptibility to erosion, piping, and other earth
45 instability issues (Elges 1985). Clays containing high exchangeable sodium percentages (ESP)
46 are usually predisposed to dispersion. The low charge of sodium ions, weakly bounded to clay
47 minerals (CRC 2001), explains such behavior. Hence, the diffuse double layer (DDL) is thicker
48 than in non-sodic soils and the repulsive forces exceed the attractive forces in saturated
49 conditions, resulting in deflocculation. Through the replacement of sodium by cations with
50 higher valence ions, such as calcium or aluminum, the potential of soil dispersivity can be
51 reduced, since the soil structure becomes denser, as a result of the reduction of the DDL
52 thickness. This condition can be achieved by the incorporation of hydrated lime (calcium
53 hydroxide) or similar additives to the soil.

54

55 Now, in presence of a dispersive sulfate-rich soils, sulfates present in various forms interact
56 with the calcium-based stabilizers, making soil susceptible to develop inconvenient pathologies.
57 Stabilizing method can lead to side problems, instead of improving original properties (e.g.,
58 Hunter 1988; Dermatas 1995; Petry and Little 1992; Kota et al. 1996; Puppala et al. 2005;
59 Puppala et al. 2010, amongst other researchers). Indeed, in hydrated and highly alkaline
60 environment ($\text{pH} > 10.5$), the alumina from clay minerals (or other source) is released into
61 solution and can react with sulfates contained in soil and/or groundwater. In these conditions,
62 it can form ettringite, which is a highly expansible calcium alumino-sulfate mineral, with a
63 needle-like structure (Mitchell and Dermatas 1992). As stated by Puppala et al. (2005), this

64 reaction continues until enough ettringite crystals are formed in the soil to produce a
65 phenomenon called sulphate-induced swelling. For temperatures below 15°C, the
66 transformation of ettringite to thaumasite (a very expansive mineral when exposed to water) is
67 possible. If the system is limited by insufficient dissolved clay ($\text{pH} < 10.5$) as well as insufficient
68 ions of either, calcium or sulphate, ettringite/thaumasite formation and expansion is terminated
69 (Dermatas 1995).

70
71 Dermatas (1995) claims there are two separate mechanisms that could be responsible for the
72 extensive sulphate-induced swelling generally associated with ettringite and thaumasite: (i)
73 crystal growth, or (ii) hydration. On the one hand, Aluminum, calcium, and sulfate ions present
74 in solution could concentrate around the ettringite nucleation sites, and combine to induce
75 ettringite crystal growth. As ettringite crystals grow, they exert significant pressures to the
76 material matrix, and if these pressures are high enough, swelling of the material can be
77 developed due to crystal growth. However, in geomaterials where void ratios are larger than
78 concrete, these crystals could be accommodated until a certain point without damaging the
79 geomaterial. On the other hand, a number of researchers, such as Mehta and Wang (1982), have
80 affirmed that the main mechanism of expansion is the adsorption of water by ettringite crystals.
81 Struble and Brown (1984) demonstrated that when ettringite is undergone to a drying-wetting
82 cycle, at 25°C, it loses about 30% of its mass upon drying. Nevertheless, when rewetting it gains
83 considerably more mass than what has been lost during drying, up to 125% of its initial mass.
84 Although, without any explanation on how this process occurs, the additional mass has been
85 attributed to adsorption of water by ettringite.

86
87 In this context, the mechanical behavior of stabilized soils can be properly assessed through
88 methods that express its overall performance by carrying out tests such as unconfined
89 compressive strength, initial shear modulus, durability and volume change due to swelling. In
90 this sense, Consoli et al. (2016) studied those parameters in a sodium rich clay treated with
91 hydrated lime and attested that it was effective in reducing the dispersivity of the soil and in
92 proportioning significant strength gains. The incorporation of a pozzolan (i.e. fly ash) with a
93 calcium-based material (i.e. hydrated lime, calcium carbide residue and lime kiln dust) in the
94 improvement of geomaterials was studied by Petchuay et al. (2016), Consoli et al. (2017, 2018),
95 Hoy et al. (2017), Arulrajah et al. (2017), among others. Jha and Sivapullaiah (2018), in turn,
96 assessed the swelling behavior of a gypseous clayey treated with lime and fly ash and verified

97 that the 20% was the optimum fly ash content in minimizing the volume change behavior due
98 to ettringite crystals growth and/or hydration.

99
100 Thus, this paper aims a better understanding of the interactions between soil from Paraguayan
101 Chaco area and calcium-based treatment, as well as to develop feasible solutions through
102 experimental tests. This issue is well recognized in the region of the Paraguayan Chaco, where
103 the effects of having such soils are persistently observed on the road infrastructure (Fig. 1),
104 which requires constant maintenance through palliative solutions. Therefore, a wider
105 comprehension of this problem and the development of feasible solutions, through experimental
106 studies, are required. An alternative treatment is the use of a pozzolanic material-lime mixture.
107 When this mixture is incorporated into the soil, it can create a cementitious matrix able to resist
108 to the swelling-induced stresses produced by the ettringite hydration and/or growth. Hence, in
109 order to assess the natural and the treated soil behavior, a thorough physical, chemical and
110 mineralogical characterization was carried out. This encompassed the influence of variables
111 (such as the dry unit weight, the lime or moisture content, the pozzolanic material content and
112 the mellowing) in the mechanical response of the treated soil. A fractional factorial design was
113 used to define the experimental plan.

114

115 **EXPERIMENTAL PROGRAM**

116

117 *Materials*

118 The soil (S), the lime (L) and the fly ash (FA) were characterized in the laboratory in order to
119 determinate their physical, chemical and mineralogical properties. The soil was classified as a
120 lean clay (CL), according to the standard ASTM D2487 (2006), and clay (A-6), according to
121 the standard AASHTO M 145 (1991). Its physical properties are presented in Table 1 and its
122 grain size distribution is shown in figure 2

123

124 The chemical analysis of pure water put in contact with soil revealed the presence of sodium
125 (44.9 mEq/l), potassium (0.2 mEq/l), calcium (15.8 mEq/l), and magnesium (4.5 mEq/l) as the
126 main released species after washing. The total soluble salts (TDS) were 65.4 mEq/l and 68.6%
127 of TDS corresponded to sodium (PS). Thus, it can be described as a potential dispersive soil as
128 stated by Sherard et al. (1976). In addition, this soil is classified as moderately dispersive (D2)
129 according to the pinhole test and dispersive (grade 4) according to the crumb test The water-
130 soluble sulphate content according to the standard ASTM C1580 (2015a), revealed the presence

131 of CaSO₄ (5,372 ppm), K₂SO₄ (93 ppm), MgSO₄ (1,351 ppm) and Na₂SO₄ (7,576 ppm),
132 corresponding to a total of 14,392 ppm of soluble sulphate salts. It is above the sulphate content
133 threshold recommended by NCHRP (2009).

134

135 Parallel to sulfate phases, X-ray diffraction pattern (Fig. 3) revealed the presence of smectite,
136 chlorite, kaolinite, illite, and quartz. The unit weight of the soil grains is 26.9 kN/m³.

137 The pozzolanic material used in this study is a coal fly ash. It is a residue produced by a thermal
138 power plant, with a mainly amorphous structure (~80%). Its main constituents are silica
139 (65.7%), alumina (20.3%) and iron oxide (4.6%). The FA particles size distribution indicates
140 that 85% of the grains are located in the silt range and 15% are distributed between the fine and
141 medium sand range. The FA grains unit weight is 20.1 kN/m³. Hydrated lime was used as an
142 alkaline activator. With a grains unit weight equal to 24.1 kN/m³, it is composed of 81% of
143 Ca(OH)₂ and 9.4% of CaCO₃ (determined stoichiometrically).

144

145 *Experimental plan*

146 The effects or coupled effects of 5 parameters (dry unit weight, lime or moisture content, the
147 pozzolanic material content and the mellowing) have to be studied. In order to reduce the
148 number of tested specimens, a half fraction factorial design – 2_v^{5-1} – was employed to define
149 the laboratory experiments regarding the stabilized dispersive sulphate-rich Paraguayan soil. In
150 this type of design (resolution V), no main effect or two-factor interaction are aliased with any
151 other main effect or two factor interactions, but main effects are aliased with four-factor
152 interactions and two-factor interactions are confounded with three factor interactions
153 (Montgomery 2009). In this sense, considering that higher order interactions were negligible
154 (sparsity effect principle), it was possible to estimate the main effects (5) and two-factor
155 interactions effects (10) through only 16 runs, without conducting a huge range of experimental
156 runs, as it would be the case if a more traditional parametrical analysis was conducted. In
157 addition, two intermediate treatments were developed, for the unconfined compression strength
158 tests, to check the linearity assumption of the model, using intermediate factors corresponding
159 to the average of the two extremes.

160

161 The measured variables were the unconfined compressive strength (UCS), the initial shear
162 modulus, the accumulated loss of mass (wet-dry durability test) and the volumetric variation.
163 The curing periods considered (28, 60 and 90 days for the UCS tests and 7 days for the
164 remaining tests) were treated as separated blocks. The varying factors were dry unit weight

165 (14.5 kN/m³ and 16.8 kN/m³), lime content (4% and 8%), molding moisture content (12% and
166 15%), the fly ash (FA) content (0% and 25%), and the mellowing time (0 h and 48 h). The latter
167 is a delay in the compaction that allows the stabilizer to diffuse through the moist soil intending
168 to anticipate the formation of the expansive minerals through the sulfates – lime reactions
169 (Rahmat and Kinuthia, 2011). Hence, those can be rearranged and/or broken during the
170 compaction, what would diminish its deleterious effects along the material's lifespan. Table 2
171 summarizes each treatment.

172

173 In addition, an analysis of the soil microstructure was carried out using scanning electron
174 microscopy (SEM) to determine the potential occurring of ettringite. The dry unit weight and
175 molding moisture content range was established based on standard Proctor compaction test
176 using standard effort in according to ASTM D698 (ASTM 2012) performed on a 4% lime-soil
177 mixture. It yielded a maximum dry unit weight and optimum moisture content of 17 kN/m³ and
178 15%, respectively.

179

180 The 4% of lime content is relative to the dry mass of soil and was defined after the minimum
181 lime amount for particle flocculation was established using the 'initial consumption of lime'
182 method (ICL). This method, thoroughly described in the literature (Rogers et al. 1997), is based
183 on the pH variation of the soil-lime blend as a function of the added lime. The pH value
184 increases with the addition of lime until a threshold value is reached and this threshold
185 corresponds to the ICL lime content. Theoretically, all the added lime beyond this point would
186 be available to promote the pozzolanic reactions, which are responsible for the most significant
187 portion of the strength increase. The results of an ICL test performed on the Paraguayan soil
188 from Chaco revealed that the minimum amount of lime is 4%. In the experimental plan, a
189 maximum lime content of 8% was chosen considering international experience (Mitchell 1981,
190 Consoli et al. 2001, 2008, 2016; Thomé et al. 2005).

191

192 The amount of fly ash was determined based on previous researches (Consoli et al. 2015;
193 Consoli et al. 2011; Kumar, Walia and Bajaj 2007; McCarthy et al. 2009, 2012; Puppala et al.
194 2001a) and calculated in relation to the weight of the dry materials (soil plus lime).

195

196 *The molding and the curing of specimens*

197 Cylindrical specimens, with 50 mm in diameter and 100 mm high, were used for the UCS tests,
198 while cylindrical specimens with 100 mm in diameter and 127 mm high were used for initial

199 shear modulus and durability tests. The volumetric expansion tests were performed with
200 cylindrical specimens with 54 mm in diameter and 21 mm high.

201 After the soil, fly ash (when used) and lime were weighed, they were manually dry blended
202 until a visual uniformity was reached. Then, distilled water was added to the mixture that is
203 blended by hand until a homogenous paste was produced. When no mellowing was imposed
204 before compaction, the mixture was immediately molded by static compaction in three layers
205 (for strength, stiffness, and durability tests) or in one layer (for volumetric expansion test), into
206 cylindrical split casts. After molding, specimens were weighed and measured with precisions
207 nearly 0.01 g and 0.1 mm in order to check the tolerances regarding the maximum variation of
208 the dry unit weight ($\pm 0.5 \text{ g/cm}^3$) and dimensions (1% of the target dimension). Then, they were
209 sealed in plastic bags and forwarded to be cured between 7 to 90 days in a humid room (95 ± 2
210 %) with controlled temperature ($23^\circ\text{C} \pm 2^\circ\text{C}$).

211
212 When mellowing was used before compaction the mixed hydrated materials were sealed in a
213 special thick plastic bag for 48 hours before proceeding to the molding. This allowed the
214 occurrence of the deleterious sulphate-calcium-alumina reactions and, hence, the possible
215 formation of ettringite before the compaction process. Thus, the formed ettringite crystals could
216 be theoretically broken and/or reallocated throughout the molding process, which would
217 minimize its harmful effects during the stabilized soil lifespan (Harris et al. 2004).

218

219 *The testing of the specimens*

220 Unconfined compression tests were carried out in according to ASTM C 39 (ASTM 2010) with
221 a loading rate equal to 1.14 mm/min. In order to minimize suction effects, the specimens were
222 immersed in water for 24 h to reduce suction (Consoli et al. 2011). All specimens were made
223 in triplicates and their characteristics are summarized in Table 2.

224

225 The initial shear modulus (G_0) of an elastic medium can be related by Eq. 1, to its specific
226 weight (ρ) and to the propagation velocity of a shear wave (V_s) through the medium. So, G_0 can
227 be quantified by measuring the velocity of an ultrasonic wave (ASTM D2845 2008). The pulse
228 velocity tests were carried out on specimens just before the durability tests.

229

$$230 \quad G_0 = \rho \times V_s^2 \quad (1)$$

231

232 In order to assess the performance of the studied (lime, FA) – soil mixtures when subjected to
233 extreme conditions, durability tests consisting in wetting-drying cycles were performed
234 following ASTM D 559 (2015). The method aims to determine the mass loss throughout 12
235 wet-dry cycles. After the 7 days curing period is completed, every cycle starts by immersing
236 the specimen in water, for 5h at $23^{\circ}\pm 2^{\circ}\text{C}$. After stove-drying for 42h at $71^{\circ}\pm 2^{\circ}\text{C}$, specimen is
237 finally brushed 18 to 20 times around its circumference and 4 times on the top and bottom
238 surfaces, by using a force of 13 N.

239

240 The swelling tests were carried out in oedometer cells (without the application of any load) in
241 accordance with ASTM D4546 (2014). Immediately after the curing period of 7 days was
242 terminated, the specimens was put in contact with water for 7 days, after the filling of the tank
243 of the oedometer cell. After this period was concluded, the specimens were oven-drying at
244 100°C for 24h, and again immersed in water for an additional 14-day period. Linear variable
245 differential transducers (LDVT) were used to record the vertical displacement of the specimen
246 during the free swelling test.

247 **RESULTS AND ANALYSIS**

248

249 The presentation pattern of results below is maintained for each test, and it consists in
250 quantitative responses in a (i) vertical bar chart graphic, the standardized effects of factors is
251 drawn in a (ii) Pareto chart graph and the first order main effects is given in a (iii) line scatter
252 plot. The bar chart graphs (i) are functional to present the magnitude of a measured parameter
253 for each experimental run (indicated in the abscissa with the corresponded treatment
254 summarized in Table 2). The Pareto chart (ii) is a useful way to show the importance and
255 statistical significance of the main effects and its interactions by plotting each factor (and
256 interactions) as a separated bar, with a magnitude equal to the standardized effect. Thus, if the
257 bar crosses the reference line, the factor is statistically significant considering the adopted
258 significance level (α). This line is the quantile $(1 - \alpha/2)$ in the Student's t-distribution and
259 depends on α , which was selected as 95%. Each factor is denoted as a letter and the second
260 order interactions are designated by the combination of the respective letters of factors. Despite
261 of its statistical significance, all main factors are shown in the Pareto graphs presented herein.
262 On the other hand, only the significant two-order interactions are presented. Line scatter plots
263 (iii) are a convenient manner to show the quantitative importance of each factor in altering the

264 measured response and are presented herein with a dotted line that indicates the average of the
265 measured variable for each test.

266

267 *Unconfined Compressive Strength*

268 Each value presented is the average of three tests in figure 4(a). The Pareto chart, presenting
269 the magnitude of the standardized effects and the reference line, is shown in figure. 4(b) and the
270 main effects plot is presented in figure 4(c). The Pareto chart shows that the addition of fly ash
271 (E), the dry density (B), and the curing period (F), are, in this sequence, the most influential
272 factors in terms of the strength development, followed by the interactions between fly ash and
273 dry density (BE), curing period and fly ash (FE), and curing period and dry density (FB). The
274 effects of the lime content (C), the mellowing time (A) and the molding moisture content (D)
275 are practically not significant for the response variable.

276

277 The highest effectiveness of the fly ash and curing period on unconfined compressive strength
278 (given by the highest slopes of the 3 points lines) can be explained by the pozzolanic reaction
279 of fly ash, available to react quickly with lime, resulting in a cementitious matrix composed of
280 calcium silicates hydrates (C-S-H) and calcium aluminates hydrates (C-A-H) (Herzog and
281 Mitchell 1963; Mateos 1961; Moh 1965). Reactions can also take place between lime and clay
282 minerals in soil. However, those reactions are slow due to the long induction period required
283 by soil particles, during which the soluble silicates and aluminates are dissolved and released
284 in the interstitial solution, to be transformed later in binding gel (Diamond et al. 1963; Müller
285 2005). Longer curing periods result in a greater consumption of lime and, thus, the precipitation
286 of more binding compounds (Müller 2005; Consoli et al. 2011, 2016).

287

288 The dry density is an indication of the compaction and interlocking between the soil grains and
289 between the soil particles, lime and fly ash. Hence, the proximity of those grains, besides
290 favoring the mechanical resistance of the mixture, favors the occurrence of both short and long-
291 term reactions (interactions BE and FB). The effects of adding different lime contents and
292 different molding moisture contents were quite small considering the range of values studied
293 herein. The mellowing time, likewise, was practically non-significant, probably due to the
294 mechanism of growth of the ettringite crystals, requiring continuous hydration to develop and
295 expand (Puppala et al. 2005; Nair and Little 2011). If those conditions were possible during the
296 curing period, swelling phenomenon and the propagation of cracks would have been observed
297 along this period.

298

299 *Pulse Velocity Tests*

300 The initial shear modulus (G_0) results, measured, before the start of durability tests, are
301 presented in figure 5. The values obtained range between 0.29 to 1.77 GPa and the higher values
302 were observed in the same treatments that presented higher unconfined compressive strength
303 results. The Pareto chart (figure 5 b) shows that only the addition of fly ash (E) and the dry
304 density (B) are significant single factors regarding the G_0 . On the other hand, the interactions
305 between lime content and fly ash (CE), molding moisture content and mellowing time (DA),
306 and dry density and fly ash (BE) are significant in altering the dependent variable response. The
307 amounts of lime (C), mellowing time (A), and molding moisture content (D) are statistically
308 insignificant. The main effects plot is presented in figure 5 (c). The reasons why the mentioned
309 variables have significant influences on the G_0 are the same that were presented for the UCS
310 tests. However, only a curing period equal to 7 days was considered in this case. The
311 significance observed in the interaction between molding moisture content and mellowing (DA)
312 can be partially explained by the high percentage of mellowing time (48 h) relatively to the
313 curing period (7 days). The mellowing time corresponds to almost 30% of the curing period.

314

315 *Durability Tests*

316 The accumulated loss of mass (ALM) registered after 12 cycles of the durability test is shown
317 on figure 6(a). The experimental runs that are omitted in this figure lost their structural integrity
318 after the first two cycles and its results contributed to the statistical analysis as an accumulated
319 loss equal to 100%. It is possible to infer that the treatments that presented higher values of
320 strength and stiffness performed better in the durability test (i.e. smaller ALM values). The
321 Pareto chart, in turn, is presented in 6(b) and the main effects plot in figure 6(c). In this
322 sequence, the addition of fly ash (E), the dry density (B) and the lime content (C) are the most
323 significant factors affecting the durability of the studied mixtures. Other factors and their
324 interactions are not influential in this response.

325

326 The addition of fly ash and a higher lime content added to soil favors the development of
327 pozzolanic reactions throughout the 12 wetting-drying-brushing cycles and it contributes to
328 enhance the performance of the compacted blends, as the test progresses (Consoli et al. 2017;
329 Saldanha et al. 2017). The dry density, as stated before, is an indicative of grains proximity,
330 their packing and interlocking. However, there is a paradox considering the compaction level
331 and the enhancement in the performance of the studied blends. At one glance, it is expected that

332 higher compaction levels imply in smaller mass losses due to the packed and interlocked
333 structure. However, if the structure is dense but with low reinforcement (low amounts of
334 additives) there is no space to comport the expansion of the minerals and the structure of the
335 specimen tends to collapse due to cracks propagation. Also, in this case, the strength of the
336 cementitious matrix is low and unable to resist the swelling of the minerals. Those are probably
337 the reasons why the specimens without the addition of fly ash and/or lower amounts of lime did
338 not performed well in the durability test, even the denser ones.

339

340 Mellowing time was not significant, probably because of the catalyzer effect during the 72°C
341 oven-drying periods, which enhances the development of the cementitious matrix. Besides the
342 improvement caused by the addition of the proposed stabilizers, the durability requirements for
343 clayey soils stated by USACE (1984) and PCA (1992), were not fulfilled. The former standard
344 allows a maximum weight loss of 6%, after twelve cycles, while the latter allows a maximum
345 loss of 7%.

346

347 *One-Dimension Free Swell Tests*

348 The volumetric variation (ΔV), obtained with a one-dimensional free swell test, is presented in
349 figure 7 (a). The larger expansion values were observed amongst the specimens where no
350 mellowing was employed and with minimum degrees of cementation due to the absence of fly
351 ash. In general, most of treatments presented volumetric variations lower than 5%, with
352 exception of 6, 7, 8, 11 and 16. The last two exhibited ΔV larger than 20%, which is probably
353 related to the lack of mellowing, no usage of fly ash and large amounts of lime (8%) prompt to
354 react with the sulfates presented in the soil forming expansive minerals. Based on expansion
355 index classification those mixtures can be classified as having expansion potential varying
356 between very low (0 – 20%) to low (21 – 50%) (ASTM 2011c) and non-expansive in according
357 to CMC (2003). Nevertheless, the selection criteria depend on infrastructure types that the site
358 soils support in the field. Low overburden structures including pavements and embankments
359 are distressed by moderate volumetric soil movements (Punthutaecha et al. 2006). Existing
360 literatures recommend a volumetric swell expansion of 5%, swelling pressure of 0.05 MPa and
361 a volumetric shrinkage strain of 17% as nonproblematic levels (Chen 1988; Nelson and Miller
362 1992; Punthutaecha 2002). Hence, the proposed treatments were effective in reducing the
363 swelling tendency, particularly in the highly cemented specimens.

364

365 The respective Pareto chart is shown in figure 7(b) and revealed that, excluding the molding
366 moisture content (D) and the lime content (C), all other factors are significant in changing the
367 response variable. Besides, the interactions between dry density and fly ash (BE), fly ash and
368 mellowing (EA), lime content and molding moisture content (CD), and dry density and
369 mellowing (BA) are also influential regarding the volumetric variation. The main effects plot is
370 presented in figure 7 (c).

371
372 The great effects observed by the use of fly ash, dry density and their interactions can be
373 explained through the enhancement in the pozzolanic reactions and, hence, in the strength of
374 the cementitious matrix, which diminishes the stabilized soil swell along the test. Indeed,
375 mellowing was significant in reducing the volume change along the experiment, probably by
376 allowing the formation of ettringite before the compaction procedure (Harris et al. 2004). The
377 significance attested in the interactions between mellowing and fly ash and mellowing and dry
378 density seem to be, as well, related to the efficiency of the cementitious matrix in encapsulating
379 the ettringite crystals when they are reallocated during the compaction procedure.

380

381 *Observation of the soil microstructure*

382 To assess the growth and formation of ettringite through a visual method, and to analyze the
383 effect of the addition of fly ash on such process, SEM images from two specimens were
384 obtained. Both specimens were molded without fly ash. The first was cured for 130 days (Figure
385 8a), while the second was the experimental run number 3 (8% of lime) submitted to the
386 durability test (Figure 8b).

387

388 In both cases the pH measurement was 10 ($\text{pH} < 10.5$), therefore, formation and expansion of
389 ettringite crystals are finished (Dermatas 1995). It is important to remark the effect of wet-dry
390 cycles as a catalyzer of ettringite growth and expansion. Firstly, a pH of 10 was reached after
391 the time of 12 wet-dry cycles (31 days) whereas in the specimen that was cured standardly the
392 pH after 30 days was 12.5 and just after 130 days was 10. Secondly, because of the facility of
393 finding ettringite in the specimen subjected to 12 wet-dry cycles during the SEM test and the
394 sizes of the found crystals in relation to the specimen cured for 130 days. This phenomenon
395 probably due to the hydration drying and rehydration of the specimens containing ettringite
396 during wet-dry test.

397

398 The SEM image presented in Figure 9, of a specimen containing 8% lime and 25% fly ash,
399 shows ettringite crystals that formed after 130 days (Figure 9a). Figure 9b is of a specimen
400 containing 8% of lime and 25% of fly ash, which was submitted to the durability test
401 (experimental run number 4).

402

403 The presence of ettringite crystals is shown less pronounced in specimens molded with lime
404 and fly ash considering the difficulty of finding ettringite and the sizes of its crystals during
405 SEM tests (Fig. 9). Ismail et al. (2012) relates that from other published studies, alkali activated
406 slag/fly ash binder systems are generally reported to have better resistance to sulfate attack than
407 Portland cement. Most of these conclusions have been drawn from changes in physical
408 appearance and compressive strength, but the mechanisms controlling this behavior on a
409 microstructural level are not yet well understood, and the analysis of sulfate resistance of
410 blended fly ash/slag binders has not previously been reported in detail.

411

412 **CONCLUSIONS**

413

414 The conclusions based on results on strength, stiffness, durability and free swell tests performed
415 on sulfate-rich dispersive expansive clay-lime and clay-lime-fly ash blends, are the following:

- 416 • Unconfined compressive strength is highly susceptible to changes in amount of
417 fly ash, dry density and curing period (in this order). This trend is compatible with
418 previous studies with fine-grained soils treated with lime and/or with lime and fly
419 ash (e.g. Consoli et al. 2011, 2016). For the range of values applied herein, lime
420 content, mellowing time and molding moisture content had negligible effects on
421 q_u .
- 422 • Considering the conditions applied in the present study, the initial shear modulus
423 seems to follow the same trend as q_u .
- 424 • The stabilization with fly ash and lime was successful in the enhancement of the
425 durability performance in comparison with the lime stabilization performance.
426 The use of fly ash and dry density were the most significant factors affecting its
427 response (Consoli et al. 2017; Saldanha et al. 2017). However, the USACE (1984)
428 and PCA (1992) requirements regarding the maximum allowable loss of mass
429 were not fulfilled.

- 430 • The creation of a more resistant cementitious matrix, through the addition of fly
431 ash, was effective in reducing the swelling during the expansion test. The
432 mellowing process was also effective in this sense, probably by the reasons stated
433 before.
- 434 • Based on the observations of SEM images, ettringite crystals appeared in treated
435 sulphate-rich Paraguayan soil. Nonetheless, crystals were more developed among
436 the durability specimen, probably due to the constant supply of water during the
437 cycles. The formation of such crystals was attributed to the presence of calcium
438 and, likewise, of reactive silica, alumina and soluble sulfates (Mitchell 1986; Nair
439 and Little 2011; Puppala et al. 2004)

440 **ACKNOWLEDGEMENTS**

441 The authors wish to explicit their appreciation to FAPERGS/CNPq 12/2014 – PRONEX (grant
442 # 16/2551-0000469-2), MCT-CNPq (Produtividade em Pesquisa) and MEC-CAPES (PROEX)
443 for the support to the research group.

444 **REFERENCES**

- 445 ASTM (2006). “Standard classification of soils for engineering purposes.” *ASTM D 2487*, West
446 Conshohocken, Philadelphia.
- 447 ASTM (2007). “Standard test method for pore water extraction and determination of the soluble
448 salt content of soils by Refractometer.” *ASTM D 4542*, West Conshohocken, Philadelphia.
- 449 ASTM (2010). “Standard test method for compressive strength of cylindrical concrete
450 specimens.” *ASTM C 39*, West Conshohocken, Philadelphia.
- 451 ASTM (2011a). “Standard specification for quicklime, hydrated lime, and limestone for
452 environmental uses.” *ASTM C 1529*, West Conshohocken, Philadelphia.
- 453 ASTM (2011b). “Standard test method for measuring deflections with a light weight
454 deflectometer (LWD).” *ASTM E 2835*, West Conshohocken, Philadelphia.
- 455 ASTM (2011c). “Standard test method for expansion index of soils.” *ASTM D 4829*, West
456 Conshohocken, Philadelphia

- 457 ASTM (2012). “Standard test methods for laboratory compaction characteristics of soil using
458 standard effort (600 kN-m/m³).” *ASTM D 698*, West Conshohocken, Philadelphia.
- 459 ASTM (2013a). “Standard test methods for identification and classification of dispersive clay
460 soils by pinhole test.” *ASTM D 4647*, West Conshohocken, Philadelphia.
- 461 ASTM (2013b). “Standard test methods for determining dispersive characteristics of clayey
462 soils by the crumb test.” *ASTM D 6572*, West Conshohocken, Philadelphia.
- 463 ASTM (2015a). “Standard test method for water-soluble sulfate in soil.” *ASTM C 1580*, West
464 Conshohocken, Philadelphia.
- 465 ASTM (2015b). “Standard test methods for wetting and drying compacted soil-cement
466 mixtures.” *ASTM D 559*, West Conshohocken, Philadelphia.
- 467 Arulrajah, A.; Mohammadinia, A.; D'Amico, A.; and Horpibulsuk, S. (2017), "Effect of lime
468 kiln dust as an alternative binder in the stabilization of construction and demolition
469 materials.", *Construction and Building Materials*, 152(October), 999 – 1007.
- 470 Chen, F. H. (1988) — Foundations on expansive soil. Elsevier. Amsterdam.
- 471 China Ministry of Construction (CMC). (2003). “Technical code for building in expansive soil
472 area.” *GBJ112-87*, Beijing: Chinese Planning Press.
- 473 Consoli, N.C.; Prietto, P.D.M.; Carraro, J.A.H.; and Heineck, K.S. (2001). “Behavior of
474 compacted soil–fly ash–carbide lime–fly ash mixtures.” *J. Geotech. Geoenviron. Engng.*,
475 127(9), 774–782.
- 476 Consoli, N.C.; Thomé, A.; Donato, M.; and Graham, J. (2008). “Loading tests on compacted
477 soil bottom ash and lime layers.” *Proceedings of the Institute of Civil Engineers –*
478 *Geotechnical Engineering*, 161(1), 29–38.
- 479 Consoli, N.C.; Dalla Rosa, A.; and Saldanha, R.B. (2011). “Variables governing strength of
480 compacted soil – fly ash – lime mixtures.” *Journal of Materials in Civil Engineering*, 23(4),
481 432–440 (DOI: 10.1061/(ASCE)MT.1943-5533.0000186).
- 482 Consoli, N. C.; Quiñónez Samaniego, R. A.; and Kanazawa Villalba, N. M. (2016). “Durability,
483 strength, and stiffness of dispersive clay–lime blends.” *Journal of Materials in Civil*
484 *Engineering*, 28(11), 04016124 (DOI: 10.1061/(ASCE)MT.1943-5533.0001632).
- 485 Consoli, N. C.; Koltermann da Silva, J.; Scheuermann Filho, H. C.; and Rivoire, A. B. (2017).
486 “Compacted clay-industrial wastes blends: Long term performance under extreme freeze-
487 thaw and wet-dry conditions.” *Applied Clay Science*, 146(September), 404-410.
- 488 Cooperative Research Center for Sustainable Sugar Production (2001). “Diagnosis and
489 management of sodic soils under sugarcane.” A *CRC Sugar Technical Publication*,
490 Townsville.

- 491 Dermatas, D. (1995). "Ettringite-induced swelling in soils: State-of-the-art". *Applied*
492 *Mechanics Reviews*, 48(10), 659-673.
- 493 Diamond, S.; White, J. L.; and Dolch, W. L. (1963). "Transformation of clay minerals by
494 calcium hydroxide attack." *Clay and Clay Minerals*, 12(1), 359-379.
- 495 Elges, H. F. W. K. (1985). "Problems in South Africa – State of the Art: dispersive soils". *The*
496 *Civil Engineer in South Africa*, 347-353.
- 497 Hayden, M. L.; and Halliburton, T. L. (1976). "Improvement of dispersive clay erosion
498 resistance by chemical treatment." *Transportation Research Record*, 536, 27 – 33.
- 499 Herzog, A.; and Mitchell, J. K. (1963). "Reactions Accompanying Stabilization of Clay with
500 Cement." *Highway Research Board*, 36, 146-171.
- 501 Hoy, M.; Rachan, R.; Horpibulsuk, S.; Arulrajah, A.; and Mirzababaei, M. (2017), "Effect of
502 wetting-drying cycles on compressive strength and microstructure of recycled asphalt
503 pavement-fly ash geopolymer." *Construction and Building Materials*, 144(July), 624-634.
- 504 Hunter, D. (1988). "Lime-induced heave in sulfate-bearing clay soils." *Journal of Geotechnical*
505 *Engineering*, 114(2), 150-167.
- 506 Ingles, O. G.; and Metcalf, J. B. (1972). "Soil stabilization principles and practice."
507 Butterworth-Heinemann Ltd, 384 p.
- 508 Ismail, I., Bernal, S. A., Provis, J. L., Hamdan, S., and van Deventer, J. S. J. (2012).
509 "Microstructural changes in alkali activated fly ash/slag geopolymers with sulfate exposure".
510 *Materials and Structures*, 46(3), 361–373
- 511 Jha, A. K.; and Sivapullaiah, P. V (2018). "Potential of fly ash to suppress the susceptible
512 behavior of lime-treated gypseous soil." *Soils and Foundations* 58(3), 654-665.
- 513 Kota, P.; Hazlett, D.; and Perrin, L. (1996). "Sulfate-bearing soils: problems with calcium-based
514 stabilizers". *Transportation Research Record: Journal of the Transportation Research*
515 *Board*, (1546), 62-69.
- 516 Mehta, S. R.; Chadda, L. R.; and Kapur, R. N. (1955). "Role of detrimental salts in soil
517 stabilization with and without cement: Effect of sodium sulphate". *Indian Concrete Journal*,
518 33(7), 336-337.
- 519 Mehta, P. K. (1973). "Mechanism of expansion associated with ettringite formation". *Cement*
520 *and Concrete Research*, 3(1), 1-6.
- 521 Mehta, P. K.; and Wang, S. (1982). "Expansion of ettringite by water adsorption". *Cement and*
522 *Concrete Research*, 12(1), 121-122.

- 523 Mitchell, J. K. (1981). "Soil improvement – State-of-the-art report." *Proceedings of the 10th*
524 *International Conference on Soil Mechanics and Foundation Engineering*, 4, 509–565.
525 Stockholm, Sweden: International Society of Soil Mechanics and Foundation Engineering.
- 526 Mateos, M. (1961). "Physical and mineralogical factors in stabilization of Iowa soils with lime
527 and fly ash." (Ph. D. thesis) Iowa State University.
- 528 Mitchell, J. K.; and Dermatas, D. (1992). "Clay soil heave caused by lime-sulfate reactions. In
529 Innovations and uses for lime". *ASTM STO 1135*, Innovations and Uses for Lime,
530 Philadelphia. 131(3), 325-337.
- 531 Moh, Z. C. (1965). "Reactions of soil minerals with cement and chemicals." *Highway Research*
532 *Board*, 86, 39-61.
- 533 Müller, C. J. (2005). "Pozzolanic activity of natural clay minerals with respect to environmental
534 geotechnics." Ph. D. Thesis, Swiss Federal Institute of Technology Zurich.
- 535 Montgomery, D. C. Design and Analysis of Experiments. 7th ed. Hoboken: John Wiley and
536 Sons, 2008, 656 p.
- 537 Nair, S.; and Little, D. (2011). "Mechanism of distress associated with sulphate-induced
538 heaving in lime-treated soils." *Journal of the Transportation Research Board*, 2212, 82-90.
- 539 NCHRP (2009). "Recommended practice for stabilization of sulphate-rich subgrade soils." The
540 National Cooperative Highway Research Program, National Academy of Sciences, 54 p.
541 (DOI: 10.17226/22997).
- 542 Nelson, J.D. and Miller, D.J. (1992). "Expansive Soils. Problems and Practice in Foundation
543 and Pavement Engineering." John Wiley and Sons, New York.
- 544 Phetchuay, C.; Horpibulsuk, S.; Arulrajah, A.; Suksiripattanapong, C.; and Udomchai, A.
545 (2016), "Strength development in soft marine clay stabilized by fly ash and calcium carbide
546 residue based geopolymer.", *Applied Clay Science*, 127-128(July), 134-142.
- 547 Petry, T. M., and Little, D. N. (1992). "Update on sulfate-induced heave in treated clays;
548 problematic sulfate levels". *Transportation Research Record*, 1362 p.
- 549 Portland Cement Association (PCA) (1992). Soil-Cement Laboratory Handbook. Skokie: PCA,
550 57p.
- 551 Premkumar, S.; Piratheepan, J.; Rajeev, P.; and Arulrajah, A. (2016). "Stabilizing Dispersive
552 Soil Using Brown Coal Fly Ash and Hydrated Lime." In: *Geo-Chicago 2016*. American
553 Society of Civil Engineers, (DOI:10.1061/9780784480144.087).
- 554 Punthutaecha, K. 2002. "Volume change behavior of expansive soils modified with recycled
555 materials." Ph.D. thesis, The University of Texas at Arlington, Arlington, Texas.

- 556 Punthutaecha, K., Puppala, A. J., Vanapalli, S. K., and Inyang, H. (2006). "Volume Change
557 Behaviors of Expansive Soils Stabilized with Recycled Ashes and Fibers". *Journal of*
558 *Materials in Civil Engineering*, 18(2), 295–306.
- 559 Puppala, A. J.; Intharasombat, N.; Vempati, R. K. (2005). "Experimental studies on ettringite-
560 induced heaving in soils." *Journal of Geotechnical and Geoenvironmental Engineering*,
561 131(3), 325-337.
- 562 Puppala, A. J.; Saride, S.; Dermatas, D., Al-Shamrani, M., and Chikyala, V. (2010). "Forensic
563 investigations to evaluate sulfate-induced heave attack on a tunnel shotcrete liner". *Journal*
564 *of Materials in Civil Engineering*, 22(9), 914-922.
- 565 Rahmat, M. N., & Kinuthia, J. M. (2011). Effects of mellowing sulfate-bearing clay soil
566 stabilized with wastepaper sludge ash for road construction. *Engineering Geology*, 117(3–
567 4), 170–179.
- 568 Rogers, C. D. F.; Glendinning, S., and Roff, T. E. J. (1997). "Lime modification of clays for
569 construction expediency." *Proc. Instn. Civ. Engrs. – Geotechnical Engineering*, 125
570 (October), 242-249.
- 571 Saldanha, R. B.; Scheuermann Filho, H. C.; Ribeiro, J. L. D.; Consoli, N. C. (2017). "Modelling
572 the influence of density, curing time, amounts of lime and sodium chloride on the durability
573 of compacted geopolymers monolithic walls." *Construction and Building Materials*,
574 136(April), 65-72.
- 575 Sherard, J.L.; Dunnigan, L.P., and Decker, R.S. (1976). "Identification and nature of dispersive
576 soils." *Journal of the Geotechnical Engineering Division*, 102(GT4), 287–301.
- 577 Sherwood, P. T. (1962). "Effect of sulfates on cement-and lime-stabilized soils". *Highway*
578 *Research Board Bulletin*, (353).
- 579 Struble, L. J., and Brown, P. W. (1984). "An evaluation of ettringite and related compounds for
580 use in solar energy storage." Progress Report, NBSIR 84-2942, National Bureau of
581 Standards, Gaithersburg.
- 582 Thomé, A.; Donato, M; Consoli, N.C., and Graham, J. (2005). "Circular footings on a cemented
583 layer above weak foundation soil." *Canadian Geotechnical Journal*, 42(6), 1569–1584.
- 584 Umesha, T. S.; Dinesh, S. V.; and Sivapullaiah, P. V. (2009). "Control of dispersivity of soil
585 using lime and cement." *International Journal of Geology*, 1(3), 8 – 16.
- 586 U.S. Army Corps of Engineers (1984). "*Flexible pavement design for airfields*." USACE
587 Technical Manual No. TM5-822-13.
- 588 Vakili, A. H.; Selamat, M. R.; Moayedi, H.; and Amani, H. (2012). "Stabilization of dispersive
589 soils by pozzolan." In: *Forensic Engineering 2012*. American Society of Civil Engineers.

590 NOTATION

591

592	G_0	<i>initial shear modulus</i>
593	q_u	<i>unconfined compressive strength</i>
594	t	<i>curing time</i>
595	V	<i>total volume of specimen</i>
596	V_s	<i>velocity of a shear wave</i>
597	γ_d	<i>dry unit weight</i>
598	ρ	<i>specific weight</i>
599	w	<i>moisture content</i>
600	ALM	<i>accumulated loss of mass</i>

601

602

603

604

605

606

607

608

609

610

611

612

613

614

615

616

617

618

619

620

621

622

623
624

Table 1 – Physical properties of the soil sample.

Parameter	Value
Liquid limit (%)	33
Plastic limit (%)	17
Plastic index (%)	16
Unit weight of the soil grains (kN/m ³)	26.9
Silt (0.002 mm < diameter < 0.075 mm) (%)	80
Clay (diameter < 0.002 mm) (%)	20
Mean particle diameter, D ₅₀ (mm)	0.065
Soluble sulfates (ppm) (ASTM C1580-15)	14,300
Sodium Absorption Ratio (SAR)	14.1
Pinhole Test (ASTM D4647 – 13)	D2
Crumb Test (ASTM D6572 – 13)	Grade 4
Soil Specific Surface Area (m ² /g)	26.2
USCS class (ASTM 2006)	CL

625
626
627
628
629

Table 2 – Experimental runs.

Experimental Run	γ_d (kN/m ³)	Lime Content (%)	FA Content (%)	Molding Moisture (%)	Mellowing Time (h)
1	14.5	4	25	15	48
2	14.5	8	25	12	48
3	14.5	8	0	15	48
4	14.5	8	25	15	0
5	16.8	4	25	12	0
6*	15.65	6	12.5	13.5	24
7*	15.65	6	12.5	13.5	24
8	16.8	4	0	15	48
9	16.8	4	25	15	0
10	16.8	8	25	12	0
11	16.8	8	0	15	0
12	16.8	4	25	12	48
13	16.8	8	0	12	48
14	16.8	8	25	15	48
15	14.5	4	0	12	48
16	14.5	8	0	12	0
17	16.8	4	0	12	0
18	14.5	4	0	15	0

630
631

*Intermediate Points



632

633 Figure 1 – Typical road pavement failure in Paraguayan Chaco.

634

635

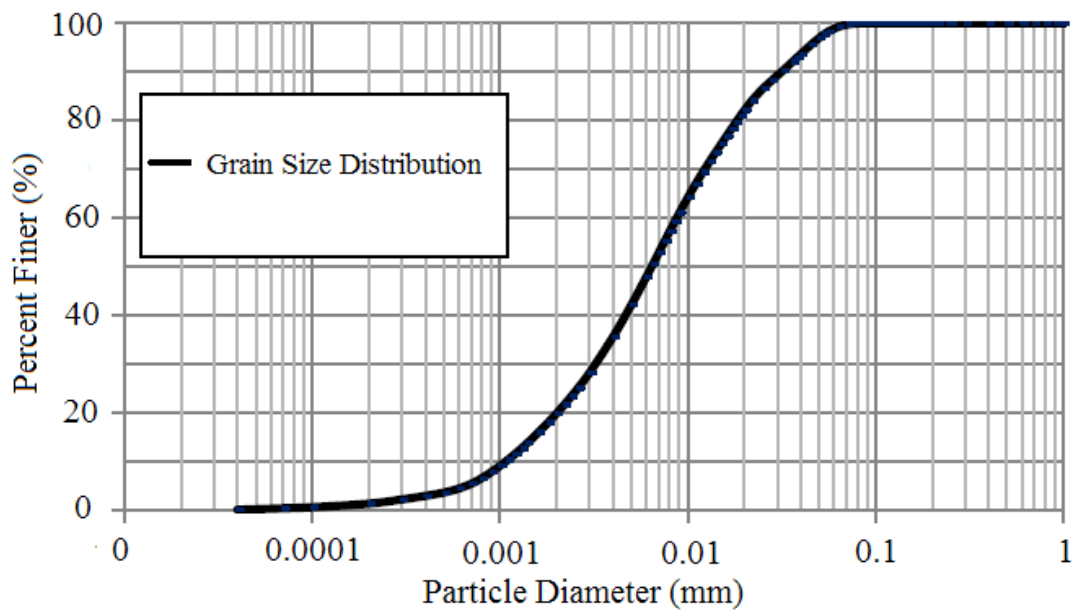
636

637

638

639

640



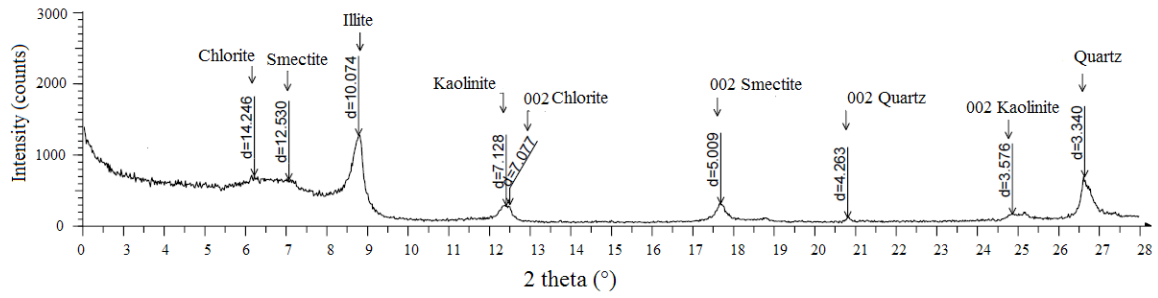
641

642 Figure 2 – Grain size distribution of the soil.

643

644

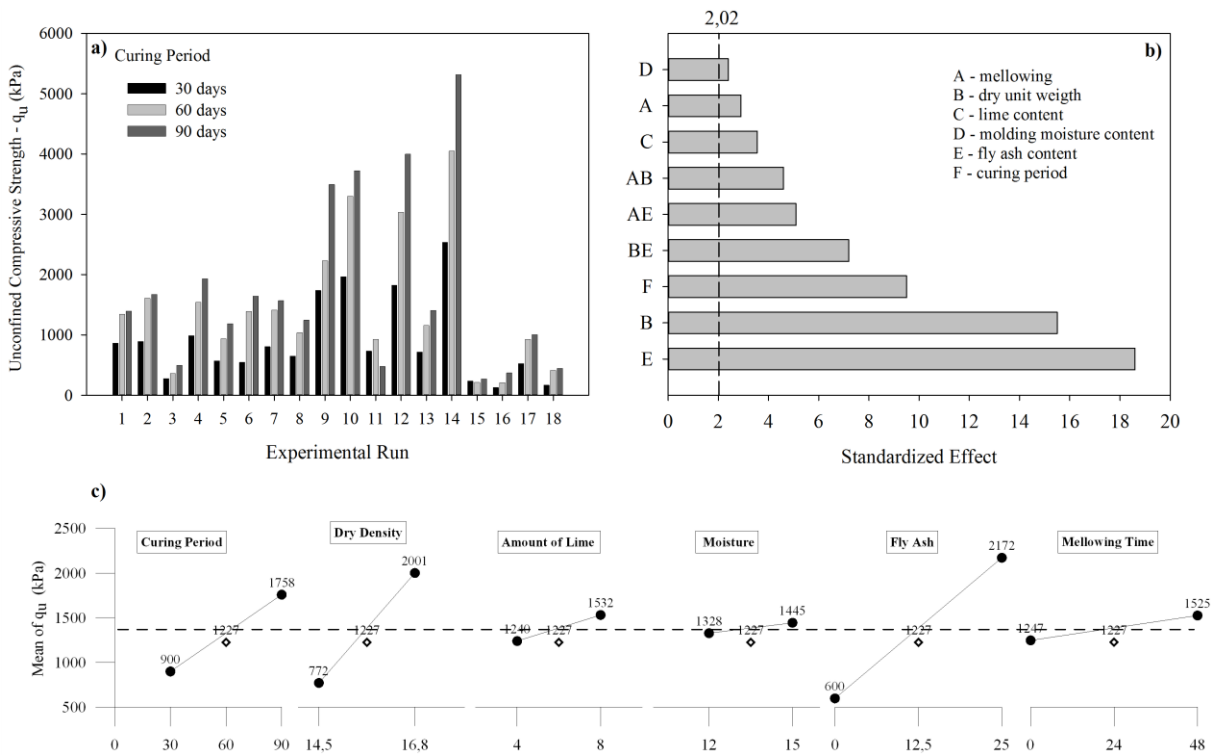
645



646

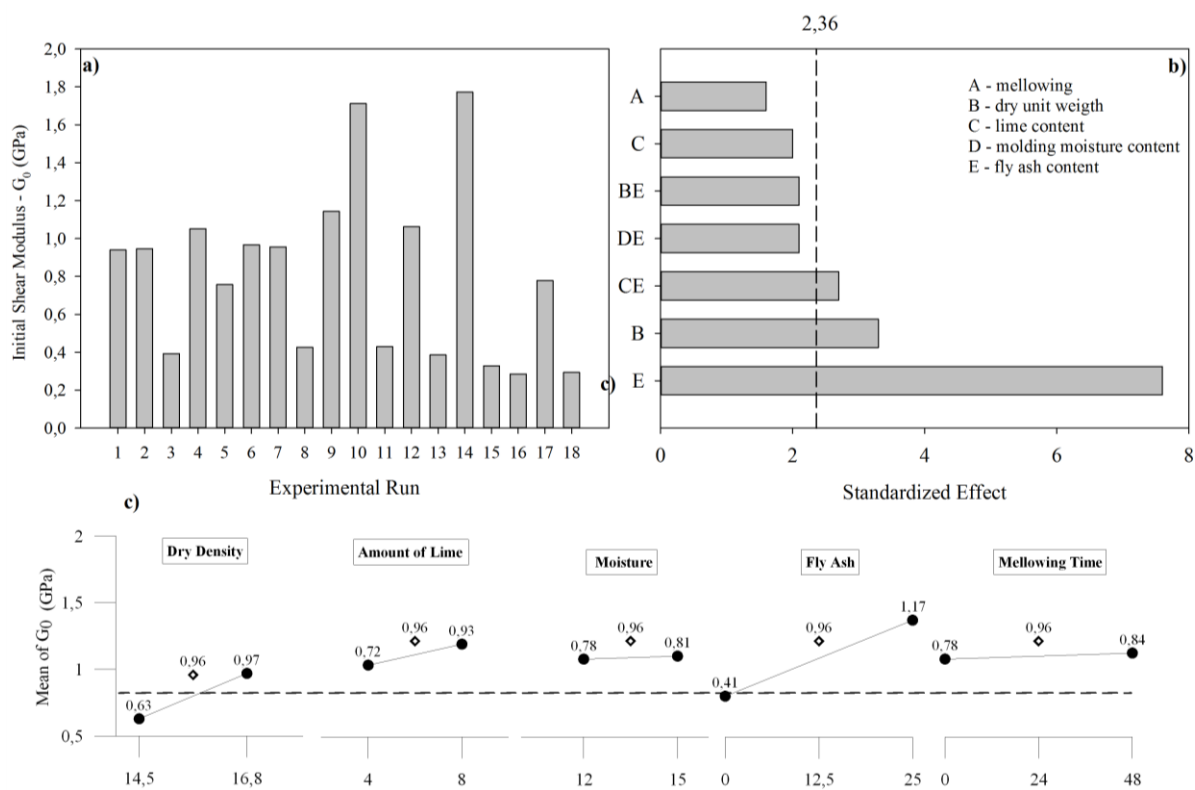
647 Figure 3 – XRD pattern of soil.

648
649
650
651
652
653
654
655
656



657

658 Figure 4 – (a) UCS results (b) Pareto Chart (c) Main effects plot.

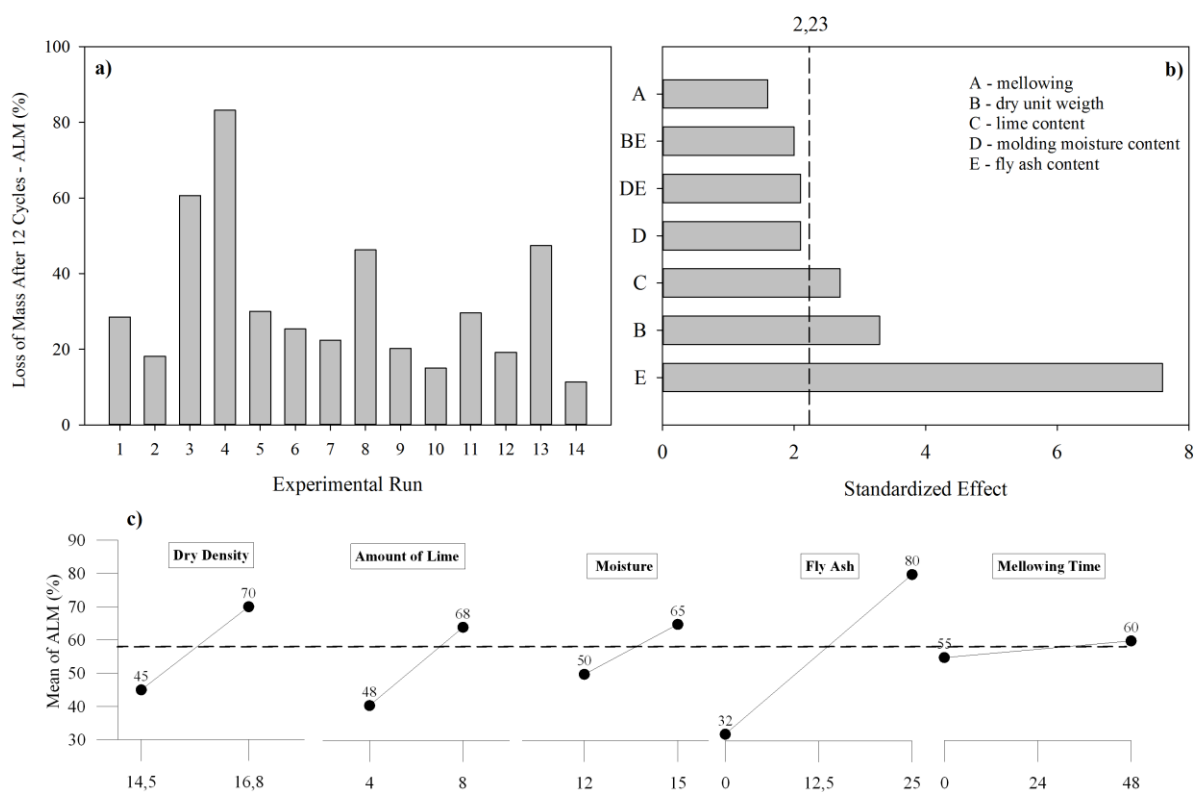


659

660 Figure 5 – (a) Pulse velocity tests results (b) Pareto Chart (c) Main effects plot.

661

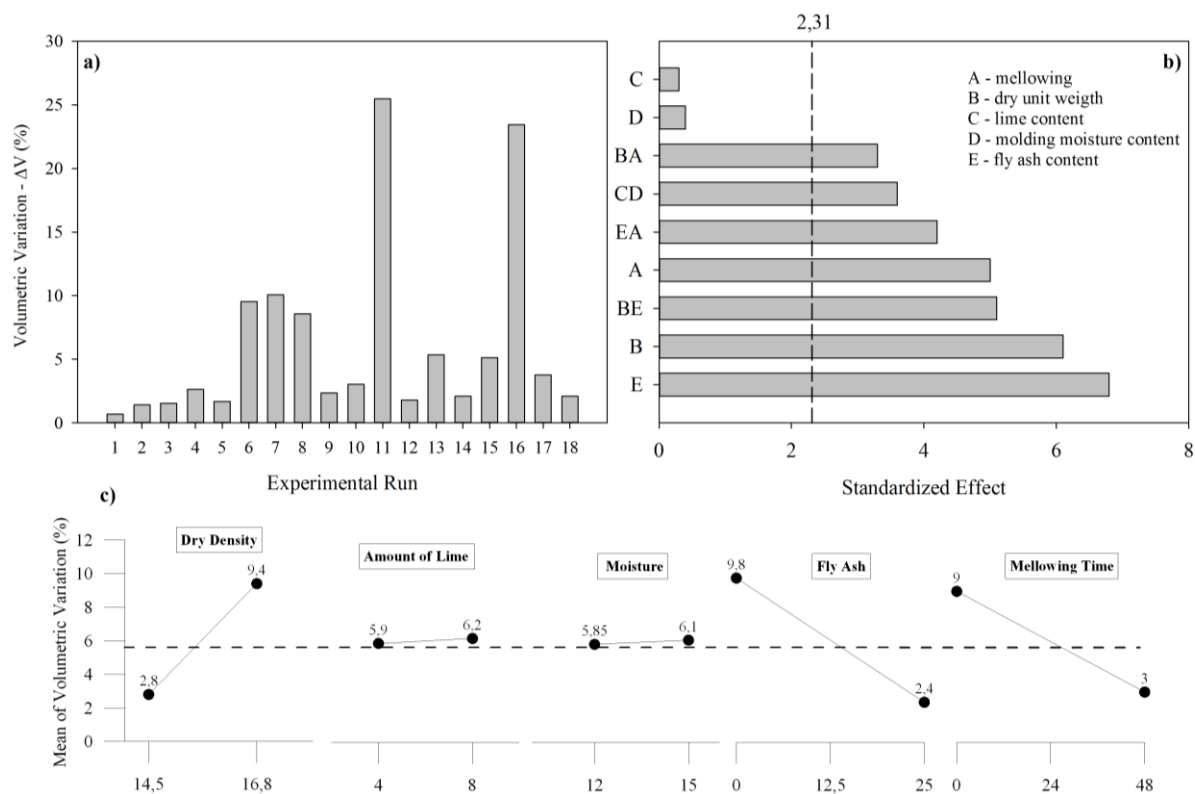
662



663

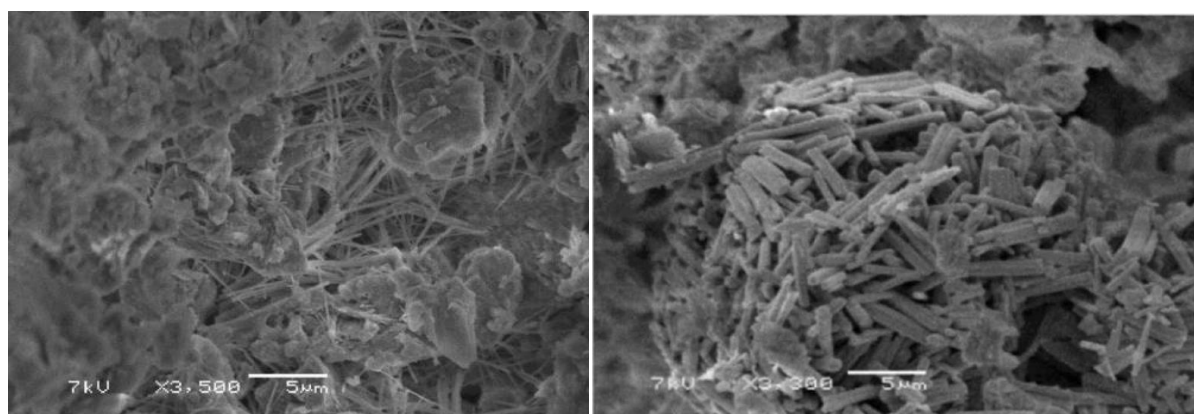
664

665 Figure 6 – (a) Durability test results, (b) Pareto Chart, and (c) Main effects plot.



666
 667 Figure 7 – (a) One –dimension free swell tests results, (b) Pareto Chart and (c)
 668 Main effects plot.

669
 670
 671
 672
 673
 674



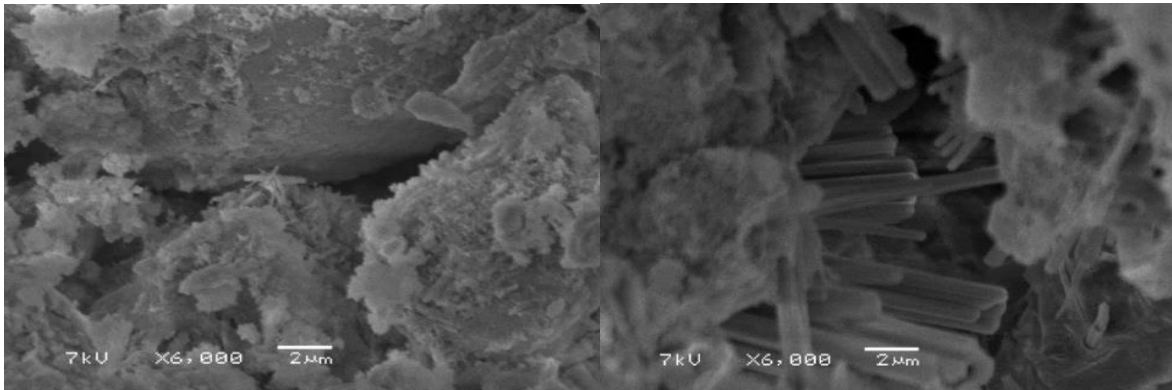
675
 676 Figure 8 - Microstructural observation by SEM without fly ash considering: (a)
 677 specimen cured for 130 days and (b) specimen subjected to 12 wet-dry cycles.

678
 679
 680

681

682

683



684

685 Figure 9 - Microstructural observation by SEM containing fly ash considering: (a)
686 specimen cured for 130 days and (b) specimen subjected to 12 wet-dry cycles.

687

688

689

690